

# Analysis of the Optical Shadow Spot Method for a Tensile Crack in a Power-Law Hardening Material

**A. J. Rosakis<sup>1</sup>**  
Research Assistant.

**C. C. Ma**  
Research Assistant.

**L. B. Freund**  
Professor and Chairman,  
Fellow ASME

Division of Engineering,  
Brown University,  
Providence, R.I. 02912

*If the crack tip deformation field in a cracked ductile solid can be characterized by means of a single plastic intensity factor, then the shadow spot method has potential as a means for direct measurement of this intensity factor. The value of the  $J$ -integral is adopted as a plasticity intensity factor, and the lateral contraction of a planar specimen of elastic-plastic power-law hardening material is calculated in terms of  $J$  from the HRR asymptotic field of elastic-plastic fracture mechanics. The theoretical caustic curve which would be generated by geometrical reflection of normally incident light from points of the deformed specimen surface lying well within the plastic zone is determined, and it is shown that the value of  $J$  is proportional to the maximum transverse diameter of the shadow spot to the power  $(3n + 2)/n$ , where  $n$  is the power hardening exponent. Synthetic shadow spot patterns obtained by numerical simulation of the optical reflection process are also shown.*

## 1 Introduction

The use of the optical shadow spot method for measuring the intensity of crack tip stress fields is now quite common in experimental work underlying the field of linear elastic fracture mechanics. The method, which is also known as the method of caustics, and some of its applications are reviewed in a recent article by Kalthoff and Beinert [1]. It was suggested in a recent paper by Rosakis and Freund [2] that the method may have potential for application in elastic-plastic fracture testing as well. This suggestion was based on the following observation. When a large plate that contains a long through-crack and which responds in a nominally manner is loaded so that crack opening occurs in the tensile mode, the stress and deformation fields very near to the crack tip assume the familiar universal spatial distributions. Only the magnitude of the near tip field varies with load and geometry, and this magnitude is customarily the mode  $I$  stress intensity factor. Within the framework of plane stress analysis, the deformed shape of the specimen surface near the crack tip is thus also known up to a scalar amplitude that is equivalent to the stress intensity factor. The success of the method of caustics is based on the fact that, with a suitable optical arrangement, the light

pattern obtained by reflecting parallel incident light from the specimen surface near the crack tip provides a direct measure of the stress intensity factor.

Once the idea of the method is described in this way, it becomes clear that applicability of the method does not hinge on the material in the crack tip region responding in an elastic manner. Instead, the key feature is that the deformed shape of the specimen surface (that is, the reflecting surface) in the crack tip region is known up to a scalar amplitude. Although the mechanics of elastic-plastic fracture is not as fully developed as elastic fracture mechanics, the available asymptotic analyses of near-tip fields in power-law hardening materials suggest that this situation may prevail for these cases as well. Within the framework of plane stress analysis, with small strains and proportional stress histories for stationary cracks, the value of Rice's  $J$ -integral has been proposed as a plastic intensity factor. The viewpoint is adopted here that  $J$  provides a suitable scalar amplitude for the deformed shape of the surface of an elastic-plastic fracture specimen, and a means of directly measuring this amplitude is discussed. While there are methods available for measuring  $J$  values for ductile materials, they apply only for rate-independent materials subjected to quasi-static loading. While the direct optical method being discussed here has drawbacks of its own, its use is not subject to the same limitations on rate of loading or material response.

In the following sections, the use of the optical method of caustics in reflection is described in a way that is more general in some respects than previous descriptions. Then, the results of asymptotic elastic-plastic crack tip analysis which lead to

<sup>1</sup>Present Affiliation: Assistant Professor, Division of Engineering and Applied Science, California Institute of Technology, Pasadena, Calif. 91125. Contributed by the Applied Mechanics Division for publication in the JOURNAL OF APPLIED MECHANICS.

Discussion on this paper should be addressed to the Editorial Department, ASME, United Engineering Center, 345 East 47th Street, New York, N.Y. 10017, and will be accepted until two months after final publication of the paper itself in the JOURNAL OF APPLIED MECHANICS. Manuscript received by ASME Applied Mechanics Division, January, 1983; final revision, June, 1983.

the so-called *HRR* field are summarized. The particular case of a power-law hardening material in a state of plane stress is examined in detail, and a relationship is derived between the value of  $J$  and the maximum transverse diameter  $D$  of the shadow spot obtained by reflection of parallel incident light from the crack tip region of the specimen surface for any value of the hardening parameter  $n$ . The complete reflected optical fields for several values of  $n$  have also been simulated for this situation, and these results show the influence of hardening on the shadow spot shapes.

## 2 Caustics in Reflection

Consider a highly polished planar specimen of uniform thickness  $d$  in the undeformed state occupying a region of the

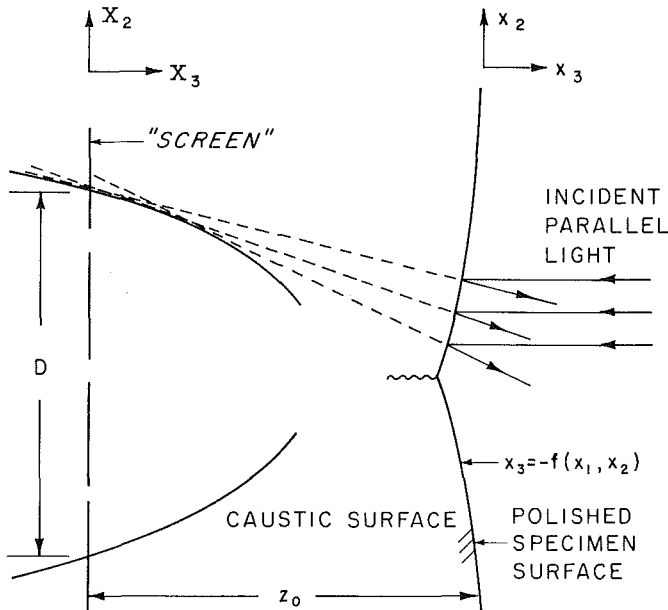


Fig. 1 Schematic diagram of the optical reflection process that results in the formation of a shadow spot pattern

$x_1, x_2$  plane. When boundary loads that tend to open the crack are applied, the resulting change in thickness is nonuniform and the equation of the deformed specimen surface is assumed to be given by

$$x_3 + f(x_1, x_2) = 0 \quad (2.1)$$

Consider a family of light rays parallel to the  $x_3$  axis incident on the reflecting surface (2.1). Upon reflection, the light rays will deviate from parallelism; see Fig. 1. If certain geometrical conditions are met by the reflecting surface, then the virtual extensions of the reflected rays will have an envelope in the form of a three-dimensional surface in space. This surface, which is called the *caustic surface*, is the locus of points of maximum luminosity (that is, highest density of rays) in the virtual extension of the reflected light field. The virtual extensions of the rays are tangent to the caustic surface. The reflected light field is recorded on a camera positioned in front of the specimen. The focal plane of the camera, which shall be called the "screen" for convenience, intersects the caustic surface at a distance  $z_0$  behind the plane reflecting surface of the undeformed specimen. On the screen, a cross section of the caustic surface is observed as a bright curve (the *caustic curve*) bordering a relatively dark region (the *shadow spot*).

If the shape of the reflecting surface and the distance  $z_0$  are specified, then the size and shape of the shadow spot can be determined. Apparently, the prescription for doing so was first presented by Manogg [3] under the assumptions that the magnitude of the surface deflection  $f$  was much less than the distance  $z_0$  and that the change in slope of the reflecting surface due to deformation was much less than unity. The analysis is only slightly more complicated if these assumptions are not invoked, it seems, and the essential steps are described in the following.

Consider that light ray that pierces the plane of the undeformed reflecting surface  $x_3 = 0$  at position  $\mathbf{x} = (x_1, x_2)$ ; see Fig. 2. This ray strikes the deformed reflecting surface at  $x_3 = -f$ , and the unit vector normal to the reflecting surface at this point, say  $\nu$ , has components  $(f_{,1}, f_{,2}, 1) / \sqrt{1 + f_{,j}f_{,j}}$  where the partial derivatives  $f_{,j}$  are evaluated at  $\mathbf{x}$  and the repeated index implies summation over  $j = 1, 2$ . Let  $\mathbf{e}_3$  denote a unit vector in the  $x_3$  direction. Then the plane that contains

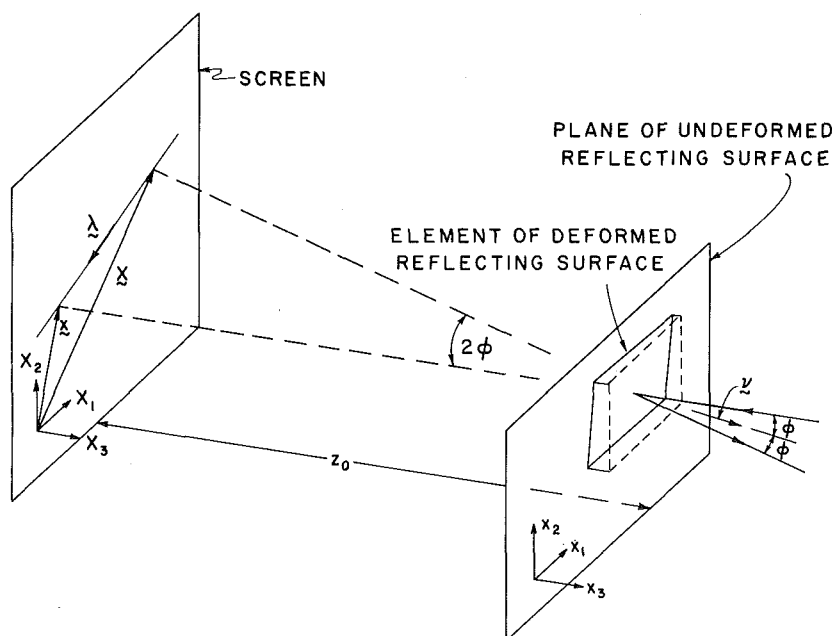


Fig. 2 Schematic diagram of the optical mapping represented by the mapping equation (2.3)

both the incident ray and the corresponding reflected ray is defined by the normal vector  $\nu \times \mathbf{e}_3$ . The intersection of this plane with the plane of the screen is then that line that has direction specified by the unit vector

$$\lambda = \frac{\mathbf{e}_3 \times (\nu \times \mathbf{e}_3)}{|\mathbf{e}_3 \times (\nu \times \mathbf{e}_3)|} \quad (2.2)$$

With this direction specified, the position  $\mathbf{X} = (X_1, X_2)$  in the screen at which the virtual extension of the reflected ray strikes the screen is

$$\mathbf{X} = \mathbf{x} - (z_0 - f) \tan 2\phi \lambda \quad (2.3)$$

where  $\phi$  is the angle between the incident ray and the normal to the reflecting surface. With this definition,

$$\tan \phi = \frac{\sin \phi}{\cos \phi} = \frac{|\nu \times \mathbf{e}_3|}{\nu \cdot \mathbf{e}_3} \quad (2.4)$$

Then, if the vector expressions are evaluated and the vector  $\nu$  is expressed in terms of its components, the optical mapping may be written in component form as

$$X_i = x_i - 2(z_0 - f) \frac{f_{,i}}{1 - f_{,j}f_{,j}} \quad (2.5)$$

If it is now assumed that  $|f| \ll z_0$  and that  $f_{,j}f_{,j} \ll 1$  then the familiar form of the optical mapping proposed by Manogg results, viz,

$$X_i = x_i - 2z_0 f_{,i} \quad (2.6)$$

Equation (2.5) or its approximation (2.6) is a mapping of the points on the reflecting surface onto the points on the screen. If the screen intersects a caustic surface in the reflected light field, then the resulting caustic curve on the screen is a locus of points for which the mapping is not invertible. That is, for those points that map onto the caustic curve, the determinant of the Jacobian matrix of the mapping must vanish. The vanishing of the Jacobian determinant is a necessary and sufficient condition for the existence of a caustic curve. The points on the plane of the undeformed reflecting surface for which the Jacobian determinant vanishes are the points from which the rays forming the caustic curve are reflected. The locus of these points on the reflecting surface is the so-called *initial curve*.

That the caustic curve is the locus of points of maximum luminosity is clear from the following simple argument. Consider incident light of uniform intensity  $q(x_1, x_2) = q_0$  measured per unit surface area on the plane of the undeformed reflecting surface. The light that passes through an arbitrary area  $\alpha$  on this plane illuminates a corresponding area  $A$  on the screen with intensity  $Q(X_1, X_2)$ . Assuming perfect reflectivity, the conservation of light energy implies that the net intensity of light on  $\alpha$  is equal to the net intensity of  $A$ , or

$$\int_{\alpha} q_0 dx_1 dx_2 = \int_A Q(\mathbf{X}) dX_1 dX_2 \quad (2.7)$$

Using the mapping (2.5) to change variables on the right-hand side, equation (2.7) becomes

$$\int_{\alpha} q_0 dx_1 dx_2 = \int_{\alpha} Q[\mathbf{X}(\mathbf{x})] B(\mathbf{x}) dx_1 dx_2 \quad (2.8)$$

where  $B$  is the determinant of the Jacobian matrix of (2.5). Because the area  $\alpha$  is arbitrary, the integrands of (2.8) are equal,

$$Q[\mathbf{X}(\mathbf{x})] = q_0/B(\mathbf{x}) \quad (2.9)$$

Thus, it is evident from (2.9) that points on the reflecting surface for which  $B = 0$  are mapped into points of maximum luminosity on the screen.

### 3 Shape of the Reflecting Surface

Most structural materials that contain cracks undergo substantial plastic deformation under rising load prior to onset of crack growth. In many cases, including standard specimen configurations, a large plastic zone develops around the crack tip and there is no region of the body over which a stress intensity factor controlled elastic field prevails. The linear elastic fracture toughness approach to fracture resistance characterization is then not applicable and other criteria, such as the critical  $J$  criterion mentioned in the Introduction, must be adopted. Methods for measuring values of  $J$  for ductile fracture specimens are available but the methods are indirect, in general, in the sense that values of  $J$  are inferred from values of other measured quantities, typically load and deflection data. In this section, attention is focused on points deep within the crack tip plastic zone, and a means of inferring values of  $J$  from the local deformation field is suggested.

Consider a large plate of elastic-plastic material that exhibits power-law hardening behavior. Suppose the plate is initially of uniform thickness  $d$  and that it contains a long through-crack. The plate is subjected to edge loading which results in a plane stress opening mode of deformation. If the midplane of the plate undergoes no transverse displacement, then the normal displacement of the plate surface  $u_3(x_1, x_2)$  is

$$u_3(x_1, x_2) = f(x_1, x_2) = \epsilon_{33} d/2 \quad (3.1)$$

where the orientation of Cartesian axes shown in Fig. 1 is assumed and  $\epsilon_{33}$  is the total strain in the thickness direction.

Hutchinson [4] and Rice and Rosengren [5] showed that the strain components in the crack tip region scale with the value of  $J$  for a power-law hardening material. They considered a monotonically loaded stationary crack in an incompressible material described by a  $J_2$ -deformation theory of plasticity and a relationship between post-yield strain  $\epsilon_{ij}$  and stress  $\sigma_{ij}$  of the form

$$\frac{\epsilon_{ij}}{\epsilon_0} = \frac{3}{2} \left( \frac{\sigma_e}{\sigma_0} \right)^{n-1} \frac{S_{ij}}{\sigma_0} \quad (3.2)$$

where

$$s_{ij} = \sigma_{ij} - \frac{1}{3} \delta_{ij} \sigma_{kk}, \quad \sigma_e^2 = \frac{3}{2} s_{ij} s_{ij} \quad (3.3)$$

and  $\sigma_0$  is the tensile yield stress,  $\epsilon_0$  is the equivalent tensile yield strain, and  $n$  is the hardening exponent. By introducing the preceding assumptions, they observed that, within a small strain formulation, a possible asymptotic strain distribution in the crack tip region is

$$\epsilon_{ij} \rightarrow \epsilon_0 \left[ \frac{J}{\sigma_0 \epsilon_0 I_n r} \right]^{\frac{n}{n+1}} E_{ij}(n, \theta) \quad (3.4)$$

as  $r \rightarrow 0$  in a polar coordinate system with origin at the crack tip. The angular factors  $E_{ij}$  in (3.4) depend on the mode of loading and on the hardening exponent. The dimensionless quantity  $I_n$ , which is defined in [4], decreases from 5 for  $n = 1$  to 2.57 for infinitely large values of  $n$  for cases of plane stress. The intensity factor  $J$  in (3.4) is the value of Rice's  $J$ -integral. The singular field (3.4) is customarily referred to as the *HRR* singularity. The asymptotic result (3.4) was derived under the further assumption that the dependence of the local field on the polar coordinates  $r$  and  $\theta$  is indeed separable.

For plane deformation, the  $J$ -integral is defined for any path of integration  $C$  by [6]

$$J = \int_C \left[ W n_1 - n_i \sigma_{ij} u_{j,1} \right] dC \quad (3.5)$$

where  $W$  is the local stress work density,  $n_i$  is a unit vector normal to  $C$ , and  $u_i$  is the particle displacement vector. The integral has the well-known property of path independence,

that is,  $J=0$  for any simple closed path in the body in the absence of body forces. This implies that  $J$  has the same value for all paths that begin on one traction-free face of a crack in a plane with normal in the  $x_2$  direction and that end on the opposite traction-free face of the crack. Because the path of integration can be chosen to be arbitrarily close to the crack tip,  $J$  has been interpreted as a measure of the strength of the crack tip singular field, a role that is obvious from the form of (3.4). Based on the observation that  $J$  is a characterizing parameter for the crack tip field, it has been suggested that a condition for onset of crack growth is the attainment of a critical value of  $J$ . This seems reasonable, provided that the one parameter characterization remains valid and that the one parameter field prevails over a region large in size compared to the fracture process zone. The interest in measuring values of  $J$  for ductile materials stems from the potential usefulness of this suggested criterion.

In view of the assumed incompressibility of material response, the strain in the thickness direction which appears in (3.1) is related to the in-plane strains by

$$\epsilon_{33} = -(\epsilon_{11} + \epsilon_{22}) = -(\epsilon_{rr} + \epsilon_{\theta\theta}) \quad (3.6)$$

For specified material parameters and a given value of  $J$ , the in-plane strains are known from (3.4), the out-of-plane strain is computed from (3.6), and the shape of the reflecting surface is then given by (3.1). Thus, for points near the crack tip, the shape of the reflecting surface is known up to a scalar amplitude, namely the plastic strain intensity  $J$ . In the next section, the relationship between the magnitude of  $J$  and the size of the shadow spot obtained by reflecting parallel incident light from this reflecting surface is established.

It should be noted that (3.6) will provide an overestimate of lateral contraction for given in-plane strains because, for most materials, the elastic part of the local deformation is not incompressible although the plastic part may be so. For points close enough to the crack tip for the plastic strain to dominate the elastic strain, however, the total strain is expected to satisfy (3.6) to an acceptable degree. An estimate of the ratio of total strain  $\epsilon_{22}$  to tensile yield strain  $\epsilon_0$  as a function of distance ahead of a crack tip in a low hardening (large  $n$ ) material may be obtained in the following way. For very large  $n$ ,  $E_{22}(n,0) \approx 0.75$  and  $I_n \approx 2.6$ . For contained plastic deformation in plane stress, the value of  $J$  is commonly related to the maximum extent of the plastic zone  $r_p$  by  $J = \pi\sigma_0\epsilon_0 r_p$ . Thus, from (3.4) for large values of  $n$ ,

$$\epsilon_{22}/\epsilon_0 \approx 0.9(r_p/r)$$

so that (3.6) is expected to provide a reasonably accurate relationship if the distance from the crack tip to the initial curve along  $\theta = 0$  is less than one-half or one-third of the extent of the plastic zone along  $\theta = 0$ .

#### 4 Shadow Patterns Associated With the HRR Field

In view of the discussion in the preceding section, the shape of the reflecting surface  $f(x_1, x_2)$  in (2.1) is given by

$$f(x_1, x_2) = \frac{1}{2}\epsilon_0 d \left[ \frac{J}{\sigma_0 \epsilon_0 I_n r} \right]^{\frac{n}{n+1}} (E_{rr} + E_{\theta\theta}) \quad (4.1)$$

Numerical values of the angular variations  $E_{ij}$  are available for many values of hardening exponent  $n$  from the work of Shih [7]. Again, equation (4.1) represents the normal displacement of points on the initially plane specimen surface due to deformation. For an initial curve that is well within the crack tip plastic zone where the HRR field can be expected to dominate, the mapping (2.6) takes the form

$$X_i = x_i + G \frac{\partial}{\partial x_i} \left[ \frac{\psi(\theta, n)}{r^{n/(n+1)}} \right] \quad (4.2)$$

where

**Table 1 Values of the numerical coefficient  $S_n$ , which appears in (4.8), from evaluation (4.9)**

$n$	$S_n$
1	0.0277
2	0.0513
3	0.0611
4	0.0660
5	0.0687
6	0.0701
7	0.0710
8	0.0715
9	0.0718
10	0.0719
15	0.0719
20	0.0717
25	0.0714

$$G = \epsilon_0 z_0 d \left[ \frac{J}{\epsilon_0 \sigma_0 I_n} \right]^{\frac{n}{n+1}}, \quad \psi = E_{rr} + E_{\theta\theta} \quad (4.3)$$

The mapping is written more conveniently in polar form as

$$\begin{aligned} X_1 &= r \cos\theta + G r^{-\frac{2n+1}{n+1}} \left[ \frac{n}{n+1} \psi \cos\theta + \psi' \sin\theta \right] \\ X_2 &= r \sin\theta + G r^{-\frac{2n+1}{n+1}} \left[ \frac{n}{n+1} \psi \sin\theta - \psi' \cos\theta \right] \end{aligned} \quad (4.4)$$

where the prime denotes the derivative with respect to  $\theta$ .

If the determinant of the Jacobian matrix of the transformation (4.4) is set equal to zero, then the result is a quadratic equation for  $r^{(3n+2)/(n+1)}$  in which the coefficients depend on  $\psi$ ,  $\psi'$ , and  $\psi''$ , as well as on the hardening exponent  $n$ . The root of the quadratic equation is

$$r(\theta, n)^{\frac{3n+2}{n+1}} = G R(\theta, n) \quad (4.5)$$

where

$$\begin{aligned} 2R(\theta, n) &= \left[ \left( \frac{n}{n+1} \right)^2 \psi + \psi'' \right] + \left\{ \left[ \left( \frac{n}{n+1} \right)^2 \psi + \psi'' \right]^2 \right. \\ &\quad \left. + 4 \frac{2n+1}{n+1} \left[ \left( \frac{n}{n+1} \right)^2 \psi^2 - \frac{n}{n+1} \psi \psi'' + \frac{2n+1}{n+1} (\psi')^2 \right] \right\}^{1/2} \end{aligned} \quad (4.6)$$

Equation (4.5) gives the initial curve on the specimen surface for a given intensity of local deformation field. Then, substitution of (4.5) into (4.2) yields the equation of the corresponding caustic curve in the  $X_1, X_2$  plane, parametric in the angle  $\theta$ ,

$$\begin{aligned} X_1 &= G^{\frac{n+1}{3n+2}} R^{\frac{n+1}{3n+2}} \left[ \cos\theta + R^{-1} \left( \frac{n}{n+1} \psi \cos\theta + \psi' \sin\theta \right) \right] \\ X_2 &= G^{\frac{n+1}{3n+2}} R^{\frac{n+1}{3n+2}} \left[ \sin\theta + R^{-1} \left( \frac{n}{n+1} \psi \sin\theta - \psi' \cos\theta \right) \right] \end{aligned} \quad (4.7)$$

for values of  $\theta$  in the range  $-\pi < \theta < \pi$ .

The shape of the caustic curve depends only on the distribution of plastic strain in the crack tip region. The absolute size of the caustic curve, on the other hand, depends on the strength of the plastic strain singularity, the bulk material properties, the geometrical parameters, and the optical parameters. In fact, equation (4.7) is a relationship among all of these parameters. Thus, if the values of the material, geometrical and optical parameters are known, then (4.7) provides a relationship between the size of the caustic curve  $D$  and the strength of the plastic singularity  $J$ . Adopting the maximum transverse diameter  $D/2 = \max(X_2)$  as the characteristic dimension, the intensity of the strain singularity can be expressed as

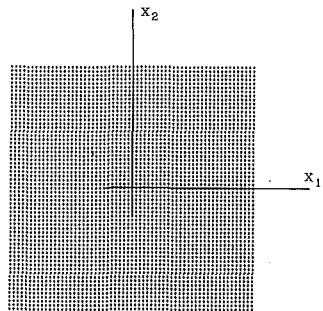


Fig. 3(a)

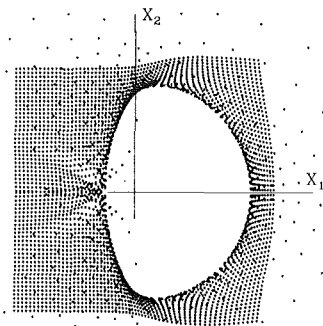


Fig. 3(e)

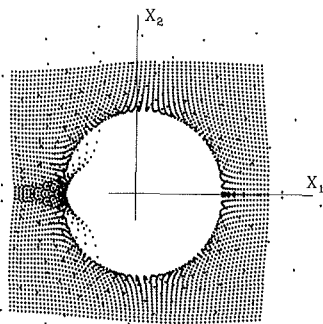


Fig. 3(b)

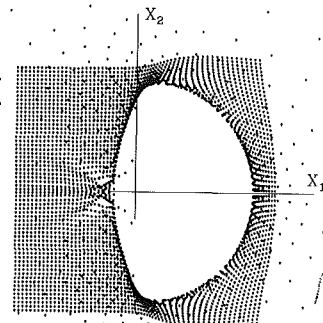


Fig. 3(f)

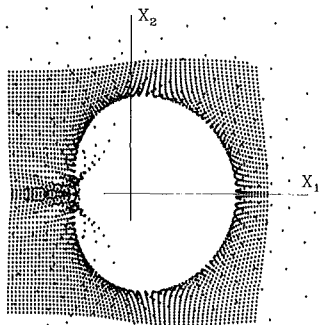


Fig. 3(c)

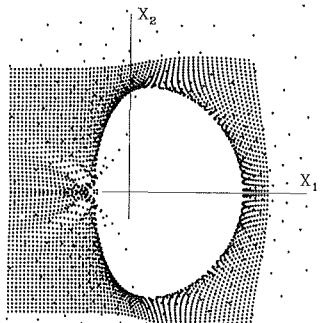


Fig. 3(d)

Fig. 3 (a) Regular array of incident light rays assumed in generating the synthetic shadow spot patterns in 3(b-f), based on the *HRR* asymptotic field. The numerical simulation of the reflection process is shown for the following hardening exponents: (b)  $n = 1$ , (c)  $n = 3$ , (d)  $n = 9$ , (e)  $n = 13$ , and (f)  $n = 25$ .

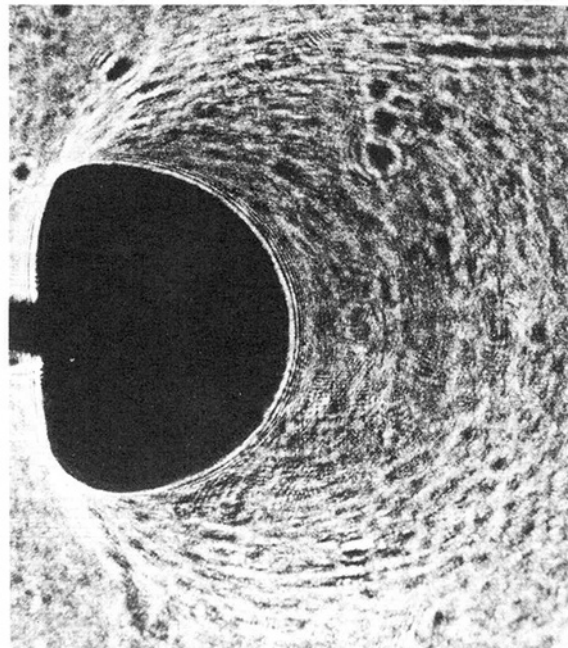


Fig. 4 Photograph of a shadow spot, surrounded by surface evidence of plastic deformation. The material is a tool steel with a low hardening rate [2].

$$J = S_n \epsilon_0 \sigma_0 \left[ \frac{1}{\epsilon_0 z_0 d} \right]^{\frac{n+1}{n}} D^{\frac{3n+2}{n}} \quad (4.8)$$

Relation (4.8) is the main result of this section. It provides a

simple relationship between the size of an observed shadow spot and the strength of the plastic singularity near the tip of the crack in an elastic-plastic power-law hardening material under conditions of plane stress.

All of the parameters that appear in (4.8) are determined

from prior knowledge of the material behavior or from the experimental set-up. The coefficient  $S_n$  is a function of  $n$  only and is given by

$$S_n = \frac{I_n}{\max_{\theta} \left\{ R^{\frac{n+1}{n}} \left[ 2\sin\theta + \frac{2}{R} \left( \frac{n}{n+1} \psi\sin\theta - \psi'\cos\theta \right) \right]^{\frac{3n+2}{n}} \right\}} \quad (4.9)$$

The expression in (4.9) has been evaluated numerically for a range of values of  $n$  from the data in [7], and the results are shown in Table 1. It is noted that for values of  $n$  greater than about 4 or 5, the value is almost indistinguishable from the asymptotic value 0.072 for large  $n$ . Further, it is noted that the limiting case of (4.8) for  $n \rightarrow \infty$  is consistent with the corresponding result for nonhardening materials which was reported in [2]. Likewise, for an elastic material ( $n=1$ ), it is well-known that the stress intensity factor  $K$  is proportional to the shadow spot diameter raised to the power  $5/2$ . That (4.8) is also consistent with this result is evident once the relationship  $J = K^2/E$ , which applies for elastic cracks under plane stress conditions, is recalled.

In order to more fully understand the phenomenon of shadow spot formation for a power-law hardening material, a companion study was carried out in which the full reflected optical field was simulated numerically. In this study, a square array of light rays was assumed to be normally incident on the surface of the specimen. The pattern in which these light rays pierce the plane reflecting surface of the undeformed specimen is shown in Fig. 3(a). These light rays were then "reflected" from a surface deformed according to (4.1), and the pattern in which the lines of the reflected rays pierce a screen positioned behind the reflecting surface was constructed. The patterns obtained for  $n=1, 3, 9, 13$ , and 25 are shown in Fig. 3. The anticipated features, such as the shadow spot (zero density of rays) and the caustic curve (high density of rays), are evident in these constructions of the reflected optical fields. Further insight into the physical process of shadow spot formation can be gained by comparing a straight row or column of rays in Fig. 3(a) to the positions into which these points map in Fig. 3(b-f). These

rows and columns map into curves that are tangent to the caustic curve at their common point, as is evident from the synthetic optical patterns.

Finally, the shadow spot photograph which appeared in [2] is reproduced here as Fig. 4 in order to illustrate the quality that might be expected in applying the ideas being proposed in laboratory testing. This photograph was produced by using light reflected from deep within the crack tip plastic zone of a tool steel with a low rate of strain hardening in the double cantilever beam configuration. It is clear from the photograph that surface evidence of plastic deformation extends far beyond the shadow spot. Some limited quantitative data are reported in [2].

### Acknowledgments

This work has been supported by the Office of Naval Research, Contract N00014-78-C-0051, and by the NSF Materials Research Laboratory, Brown University.

The computations were performed on the VAX-11/780 Engineering Computer Facility at Brown University. This facility was made possible by grants from the National Science Foundation (Solid Mechanics Program), the General Electric Foundation, and the Digital Equipment Corporation.

### References

- 1 Beinert, J., and Kalthoff, J. F., "Experimental Determination of Dynamic Stress Intensity Factors by the Method of Shadow Patterns," in *Mechanics of Fracture*, Sih, G. C., ed., Noordhoff, Leyden, 1979.
- 2 Rosakis, A. J., and Freund, L. B., "Optical Measurement of the Plastic Strain Concentration at a Crack Tip in a Ductile Steel Plate," *ASME Journal of Engineering Materials and Technology*, Vol. 104, 1982, pp. 115-120.
- 3 Manogg, P., "Anwendung der Schattenoptik zur Untersuchung des Zerreisvorganges von Platten," Doctoral Dissertation, University of Freiburg, 1964.
- 4 Hutchinson, J. W., "Singularity Behavior at the End of a Tensile Crack," *Journal of the Mechanics and Physics of Solids*, Vol. 16, 1968, pp. 13-31.
- 5 Rice, J. R., and Rosengren, G. F., "Plane Strain Deformation Near a Crack Tip in Power Law Hardening Materials," *Journal of the Mechanics and Physics of Solids*, Vol. 16, 1968, pp. 1-12.
- 6 Rice, J. R., "Mathematical Analysis in the Mechanics of Fracture," in *Fracture: An Advanced Treatise II*, Liebowitz, H., ed., Academic Press, 1968, pp. 191-311.
- 7 Shih, C. F., "Elastic-Plastic Analysis of Combined Mode Crack Problems," Ph.D. Thesis, Harvard University, 1973.